JOURNAL OF CATALYSIS 142, 237–253 (1993)

Preparation of Promoted Platinum Catalysts of Designed Geometry and the Role of Promoters in the Liquid-Phase Oxidation of 1-Methoxy-2-propanol

T. MALLAT,* Z. BODNAR,* A. BAIKER,*,[1] O. GREIS,† H. STRÜBIG,† AND A. RELLER‡

*Department of Chemical Engineering and Industrial Chemistry, Swiss Federal Institute of Technology, ETH-Zentrum, CH-8092 Zürich, Switzerland; †Electron Microscopy Laboratory, Technical University Hamburg, 2100 Hamburg 90, Germany; and ‡Institute of Inorganic and Applied Chemistry, University of Hamburg, 2000 Hamburg 13, Germany

Received July 28, 1992; revised March 15, 1993

Alumina-supported or unsupported M/Pt-type catalysts were prepared by consecutive reduction of Bi, Pb, Sn, Ru, Au, or Ag modifiers (M) onto Pt particles. Structural and chemical properties of the bimetallics were studied by electron microscopy combined with energy dispersive X-ray analysis and an electrochemical (cyclic voltammetric) polarization method. Preferential deposition of promoter metal submonolayers on Pt was observed at moderate surface coverages ($\theta_M < 0.5$–0.8). Some bulk metal crystallite formation as "bridges" between small Pt particles covered partially with promoter was also observed on alumina-supported Bi/Pt and Pb/Pt catalysts. Measurement of the electrochemical potential of the catalyst slurry during the oxidation of 1-methoxy-2-propanol to methoxyacetone and the cyclic voltammetric polarization of the bimetallic catalysts revealed that the catalysts are in an oxidized state during reaction. The following order of promoting influence was observed: Bi > Pb ~ Sn > Au ~ Ru. Two major effects of promoters are suggested: (i) they suppress the initial irreversible adsorption of the reactant alcohol on Pt which results in self-poisoning, and (ii) they form new active centers that adsorb the oxidizing species (OH) better than Pt. A formal rate equation is suggested ($r = f \cdot \theta_{org} \cdot \theta_{(OH)}$) which explains the optimum in promoter/platinum ratio. The different influences of the promoters are explained by their hydrogen and oxygen sorption characteristics and by the surface geometry of the bimetallic catalysts.

INTRODUCTION

An increasing number of papers have been published in the last decade on the liquid-phase oxidation of alcohols with promoted platinum and palladium catalysts (*1–14*). The promoting components of the bi- or trimetallic catalysts alone are inactive in the oxidation reactions. Pb or Bi have been applied mostly, but many others including Cd, Tl, Co, Ag, Te, Se, Ce, and Sn have been found advantageous to increase the reaction rate or selectivity and eliminate catalyst deactivation.

There are very few data in the catalytic literature concerning the location and chemical state of the promoter and the mechanism of promotion. The catalysts are usually prepared by deposition of the promoter onto the surface of supported noble metal catalysts in the form of hydroxides or phosphates. In the oxidation of D-gluconic acid to 2-keto-D-gluconic acid the authors could only prove that the lead–phosphate promoter is "closely associated" with platinum (*3*). The change in selectivity was attributed to the Pb^{2+}-complexation with the substrate.

A transmission electron microscopic study combined with energy dispersive X-ray analysis (TEM-EDX) of a Pd–Pt–Bi/C catalyst prepared by coprecipitation revealed the existence of separate bismuth phases in the form of well-crystallized Bi_2O_3

[1] To whom correspondence should be addressed.

0021-9517/93 $5.00

and $Bi_2O_2CO_3$ rods (*4*). Palladium and bismuth were found mainly in the oxidized state and platinum in the reduced one by ESCA and SIMS investigations. There was no detectable interaction between Bi and the noble metals and the role of Bi in the selective oxidation of glucose to gluconic acid remained unclear.

In some cases the promoted catalysts were prepared in situ by a simple addition of the promoter salt to the reaction mixture before the reaction (*1, 6*). In the oxidation of alcohols only the Pt^0 or Pd^0 sites are active, therefore a prereduction step before the oxidation reaction is generally applied. We have found by STEM, XPS, XRD, AAS, and electrochemical polarization methods that during the prehydrogenation of a palladium on carbon catalyst promoted with lead acetate, most of the Pb^{2+} was reduced to Pb^0 (*10–12*). Lead was deposited on the palladium surface as bulk metal and adatom, and on the carbon support as bulk metal. The reaction studied was the partial oxidation of 1-methoxy-2-propanol to methoxyacetone in aqueous NaOH:

$$CH_3O\text{–}CH_2\text{–}CH(OH)\text{–}CH_3 + \tfrac{1}{2}\,O_2 \rightarrow CH_3O\text{–}CH_2\text{–}CO\text{–}CH_3 + H_2O. \quad (1)$$

During the oxidation reaction bulk lead partially dissolved as Pb^{2+}, while lead adatoms remained virtually unaltered. The main role of lead and bismuth promoters was the suppression of by-product formation and their strong adsorption on the active sites.

From these results we concluded that supported palladium or platinum catalysts modified by a submonolayer of heavy metals on the noble metal particles should have better catalytic performances than those having both adatoms and metallic (bulk) deposits. Moreover, the interpretation of the results and the identification of the role of promoter may be easier in the former case. For the present study the catalysts were prepared by consecutive reduction of the promoter metal onto the surface of a commercial platinum on alumina catalyst. The structure of the catalysts has been investigated by a combined electron microscopic–X-ray analytical method and an electrochemical polarization method (cyclic voltammetry).

The oxidation state of a catalyst used in redox reactions can reliably be detected with *in situ* methods. The measurement of the catalyst potential during reaction is the only method to our knowledge which provides this type of information from a solid–liquid–gas phase system. The method has been extensively used by Russian scientists in studying catalytic hydrogenations in slurry reactors (e.g., (*15*)). Here we apply it in combination with an electrochemical polarization method (cyclic voltammetry) to study the role of promoters in the oxidation reaction.

EXPERIMENTAL

Catalysts

Distilled water (after ion exchange) and purum or puriss grade reagents were used for the experiments. For the preparation of an unsupported platinum powder 12 mmol H_2PtCl_6 in 100 ml water was dropped into 300 ml 0.4 *M* aqueous $NaHCO_3$ solution at 95°C. After refluxing it for 3 h the slurry was cooled to 30°C and treated with hydrogen for 3 h. The metal dispersion was 0.052 determined from the hydrogen region of a cyclic voltammogram (*16*). The alumina-supported platinum was a commercial catalyst of 5 wt% metal loading (Engelhard 4462). The metal dispersion (D = 0.30) was determined from the TEM pictures.

The bimetallic catalysts were prepared by consecutive reduction of the promoter metal onto the surface of platinum. Before promotion the noble metal catalyst was prereduced in water (50–100 ml/g catalyst) with hydrogen. The pH was decreased to 3 with perchloric acid (unsupported Pt) or acetic acid (alumina-supported Pt, to avoid the corrosion of alumina) and the appropriate amount of bismuth nitrate, lead acetate, tin chloride, ruthenium chloride, gold chloride, or silver acetate in a dilute aqueous acetic acid solution (10^{-3}–10^{-4} *M*, pH = 3) was dropped into the mixed slurry in 15–20 min, in a

hydrogen atmosphere. By this way the actual promoter metal ion concentration was around 10^{-6} *M* in the thoroughly mixed slurry. The metal composition of the catalysts was determined by atomic absorption spectroscopy (AAS).

Oxidation Procedure

The reactions were performed in a 200-ml flat-bottomed, thermostated glass reactor (D = 75 mm) equipped with gas inlet and outlet, reflux condenser, thermometer, and measuring and reference electrodes. The mixing frequency of the magnetic stirrer was 1500 min^{-1}; the length of the magnetic rod was 50 mm. The system was initially flushed with nitrogen, then 450 mg catalyst in 30 ml water was treated with hydrogen for 20 min, at room temperature; 50 mmol 1-methoxy-2-propanol and 3 mmol borax were added after flushing with nitrogen. The reaction temperature was 30°C. The air flow rate (25 ml · min^{-1}) was measured by a rotameter. Product analysis was carried out during and after reaction using a gas-chromatograph (HP 5890). Details of the analysis and the identification of the by-products can be found elsewhere (*10*, *17*).

A preliminary kinetic analysis revealed that the reaction rate was generally limited by the rate of oxygen supply. This situation was necessary to avoid the over-oxidation of the active sites. The rate of the surface chemical reaction decreased with increasing conversion due to the lower substrate concentration and to deactivation processes. At a certain conversion the chemical reaction becomes the rate-limiting one, and the active sites are rapidly oxidized and the catalyst is deactivated. The different final conversions achieved with various catalysts in otherwise identical reaction parameters is an indication of the different activities (rate of the surface chemical reaction) in the oxidation reaction.

Electron Microscopy

Preliminary morphological investigations were performed by analytical scanning electron microscopy (SEM) using a JEOL JSM 840A system equipped with an energy dispersive X-ray analysis (EDX) facility LINK AN 1055S with a windowless Si/Li detector system. The samples were disposed on a conductive polycarbonate film which was mounted on an aluminium target.

High-resolution transmission electron microscopy (HRTEM) and selected area electron diffraction were carried out using a JEOL 200 CX microscope equipped with a top-entry stage. For the microanalytical investigations, scanning transmission electron microscopy (STEM) was used (JEOL 2000 FX II). For elemental analysis, an energy dispersive X-ray spectrometer LINK AN 1085S with an Si/Li detector system separated with an ultrathin window was used. The samples were gently ground and dispersed in hexane, acetone, or a mixture of hexane/methanol. The slurry was disposed on a holey film of amorphous carbon supported on a copper grid.

For the determination of metal dispersion of the alumina supported platinum catalyst, different fields were examined and about 1000 particles were counted and their size determined. The degree of dispersion was calculated from the surface average diameter (*18*).

Electrochemical Methods

All the potentials in the paper are referred to an $Ag/AgCl/KCl_{(sat)}$ electrode (E = 197 mV). The electrochemical cell and polarization method used for cyclic voltammetric measurements have been described previously (*12*); 2 mg catalyst powder on a carbon paste electrode was polarized with 1 mV · s^{-1} scan rate in 0.1 *M* aqueous borax or NaOH solutions. The degree of coverage of platinum surface by the promoter atoms, θ_M is defined as

$$\theta_M = (N_{H,0} - N_{H,M})/N_{H,0}, \qquad (2)$$

where $N_{H,0}$ and $N_{H,M}$ are the number of adsorbed hydrogen atoms on surface platinum atoms (Pt_s) in the absence and in the presence of promoter, respectively.

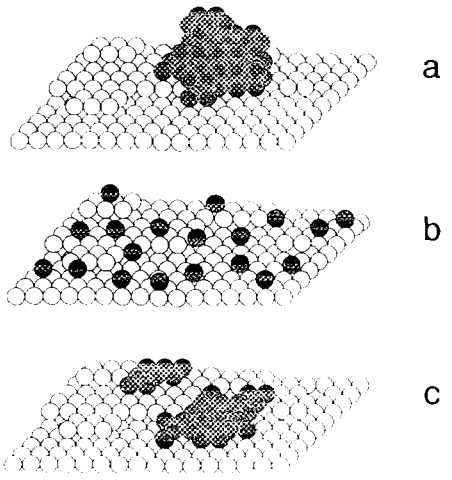

FIG. 1. Schematic representation of different promoter (grey) deposition on platinum (white) particles: (a) bulk (metallic) crystallite, (b) isolated adatoms, and (c) adatoms in big clusters.

The electrochemical potential of the catalyst, which was considered as a slurry electrode, was measured with a Pt rod electrode (Metrohm) during the oxidation reaction. The reference electrode was an Ag/AgCl/$KCl_{(sat)}$ electrode (Metrohm). More details of the method can be found elsewhere (*15, 19, 20*).

RESULTS AND DISCUSSION

1. Surface Structure of the M/Pt-Type Bimetallic Catalysts

For the study of the role of modifying components in alcohol oxidation several unsupported and alumina-supported platinum catalysts with M = Bi, Pb, Sn, Ru, Au, and Ag modifiers have been prepared. Our aim was to approach an ideal surface geometry where the modifier forms a submonolayer on the surface of platinum. In general, the second component of a bimetallic catalyst prepared by consecutive reduction may be deposited as bulk metal particles, isolated adatoms, and/or adatom islands (Fig. 1). It is expected that metal adatoms, especially the isolated ones, have higher influence on the catalytic performances than bulk metallic crystallites. There are several examples in the electrocatalytic literature (e.g., (*21, 22*)) on the preparation of platinum or other noble metal catalysts modified by foreign metal adatoms. Most of these methods are based on thermodynamic considerations: the deposition of a foreign metal submonolayer takes place at more positive potentials than the Nernst potential of bulk metal deposition ("underpotential deposition," UPD). Here we apply a nonelectrochemical method. Our approach is based on kinetic considerations. It was found that if both adatom and bulk metal deposition (in our case the formation of Pt–M and Pt–M–M bonds) is possible thermodynamically, a submonolayer deposition is favourable from very dilute (10^{-4}–10^{-6} *M*) solutions. These conditions may easily be set up by a slow dosing of the metal salt solutions into the catalyst slurry. We have found in an optimization procedure that the proper choice of reducing agent (hydrogen), metal ion concentration ($\sim 10^{-6}$ *M*), pH (~3), and nature of anions (acetate) permits the preferential deposition of several promoters onto alumina-supported platinum particles as adatoms.

It is difficult to verify the presence of a monolayer or submonolayer of foreign metal adatoms and to distinguish this structure from bulk metallic crystallites on platinum. In many cases XPS does not show any difference in binding energies (*11*) and the reliable interpretation of the data needs conductive substrates (*23*). The latter limitation exists also for the electrochemical polarization method (cyclic voltammetry), but the advantage of this method is that the differences in binding energies of the M_{ad}/Pt and M_{bulk}/Pt structures are excellently shown (*21, 22*). Unique features of the electrochemical polarization method are that (i) the same aqueous alkaline solution may be applied for the study of the surface structure of the catalyst and for the liquid-phase oxidation of the alcohol substrate and (ii) it permits the study of hydrogen and oxygen sorption on the bimetallic particles in aque-

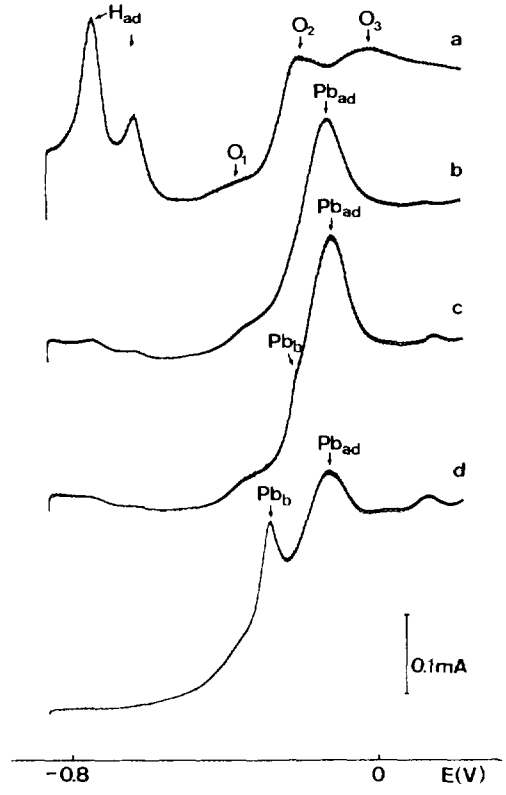

FIG. 2. Positive sweeps of the cyclic voltammograms of Pt (a) and Pb–Pt (b)–(d) catalyst powders in 0.1 *M* NaOH, with 1 mV · s^{-1} scan rate; (b) θ_{Pb} = 0.80, (c) θ_{Pb} = 0.88, and (d) θ_{Pb} = 1.0.

ous solutions, without any pretreatment of the catalyst.

Unsupported M/Pt catalysts. The cyclic voltammograms of all the unsupported bimetallic catalysts have been measured in dilute aqueous alkaline solutions. The positive sweeps of the voltammograms of the lead-modified platinum catalysts, as examples, are shown in Fig. 2. Curve (a) represents the polarization of unmodified platinum in 0.1 *M* aqueous NaOH. The ionization of adsorbed hydrogen between −0.86 and −0.45 V and the surface oxidation of platinum above −0.45 V slightly overlap. O_1, O_2, and O_3 correspond to the adsorption of OH species up to monolayer coverage (*24*). A new peak on curve (b), at −0.12/−0.15 V indicates the oxidation of a submonolayer of lead adatoms (*25*, *26*). Lead does not adsorb hydrogen, thus θ_{Pb} may be calculated from the change in hydrogen sorption (θ_{Pb} = 0.80). The site requirement of a lead adatom is 2, but this value decreases with increasing coverage and the Pb_{ad}/Pt_s ratio cannot be reliably calculated from θ_{Pb}.

A further increase of lead content of the bimetallic catalyst (θ_{Pb} = 0.88, curve (c)) resulted in the appearance of bulk lead as a shoulder at −0.2/−0.25 V. If a platinum powder is simply mixed with hydrogen in the presence of lead–acetate (Pb/Pt_s = 2.0), both adsorbed and bulk (metallic) lead are deposited onto the platinum surface (curve (d)). Note that the position of the peak corresponding to the oxidation of bulk lead was found to be strongly dependent on the pH, on the nature of anions and on the relative amount of bulk and adsorbed lead.

A detailed study of bismuth deposition onto platinum led to similar results, though bulk metal deposition was observed from a lower surface coverage on ($\theta_{Bi} > 0.5$). We can conclude that our preparation method permits the deposition of a sub-monolayer of foreign metal adatoms on unsupported platinum up to a relatively high coverage.

Alumina-supported M/Pt catalysts. When supported bimetallic catalysts are prepared by consecutive reduction of the promoter metal, a further difficulty is to avoid bulk metal deposition onto the support of high surface area. An advantage of applying hydrogen as reducing agent is that only platinum metal ions may be reduced at room temperature in the absence of another platinum metal. The reduction of, e.g., bismuth or lead ions necessitates the presence of platinum. Metal deposition occurs with the simultaneous ionization of preadsorbed hydrogen on platinum (*23*):

$$M^{n+} + nH_{ad} \rightarrow M_{ad} + nH^{+}. \qquad (3)$$

In general, hydrogen adatoms can spill over from the platinum particles to the surrounding support and reduce some of the metal ions. The thermodynamic possibility

of reducing a metal ion by hydrogen in aqueous solutions can be calculated using the Nernst equation. In case of bismuth, which was found to be the best promoter in the partial oxidation of several alcohols, bulk metal deposition either onto platinum or onto the support cannot be excluded thermodynamically. A detailed electrochemical interpretation of bulk metal and adatom deposition can be found elsewhere (*21*, *22*). Nevertheless, the deposition of the modifying metal onto the support could be suppressed by a proper selection of the reaction variables applying moderately acidic, very dilute solutions at 25°C. The method cannot be simply adopted to carbon supported catalysts. In the presence of a support of good electric conductivity the ionization of adsorbed hydrogen on the platinum surface and the discharge of the promoter metal ion on the carbon support may by locally separated, resulting in large bulk metal crystallites on the support (*11*):

$$M^{n+} + ne^- \rightarrow M_{bulk} \qquad (3a)$$

$$H_{ad} \rightarrow e^- + H^+. \qquad (3b)$$

The surface structure of the alumina supported platinum catalysts before and after promotion was characterized by electron microscopy. The electron micrograph of the unmodified 5 wt% platinum on alumina catalyst at relatively low magnification is shown in Fig. 3. The crystalline alumina flakes are covered by high-contrast platinum crystallites. The diameter of the alumina flakes is in the range of a few μm. The corresponding electron diffraction pattern reveals that the alumina support is highly crystalline. Due to the relatively low platinum concentration no corresponding electron diffraction (ring) pattern is observable.

Electron micrographs of the platinum catalyst taken at higher magnifications show small and usually isolated Pt crystallites dispersed on the alumina support (Fig. 4). The alumina support is made up of highly crystalline domains, which are mutually oriented. This explains the observed pseudo-single-crystalline electron diffraction pattern (Fig. 3). The average diameter of the platinum crystallites is between 3 and 4 nm, and the size distribution is rather narrow. The shape of the crystallites is very regular. In many cases fringes of the crystallographic planes and facetting can be observed. This indicates the presence of small platinum single crystals.

The platinum on alumina catalysts promoted with lead or bismuth are partly made up of crystallites as described for the unpromoted catalyst and partly consist of agglomerated crystallites. These agglomerates reach diameters of 10–20 nm. Again, fringes of crystallographic planes can be observed. A metric comparison between fringes of the crystallites of bimetallic catalysts and the ones of undoped platinum does not lead to unambiguous results, i.e., the formation of an alloy phase adopting different crystallographic cell constants cannot be proven.

In Fig. 5, a high-resolution electron micrograph of a bismuth-promoted platinum catalyst (Bi/Pt = 0.06) is shown. In the upper right corner crystallites are present, which are comparable to those found for the unmodified platinum. These type of particles represent the main portion of the bimetallic catalysts. In the center region of the alumina support flake agglomerated crystallites with round edges are shown.

The compositional characterization of the particles were made by analytical investigations (STEM-EDX). When the diameter of the analyzed array was in the range of >100 nm, the nominal ratio between promoter and platinum could be confirmed within an error explicable by methodological and synthetic

FIG. 3. Electron micrograph and corresponding electron diffraction pattern (insert) of the 5 wt% platinum on alumina catalyst.

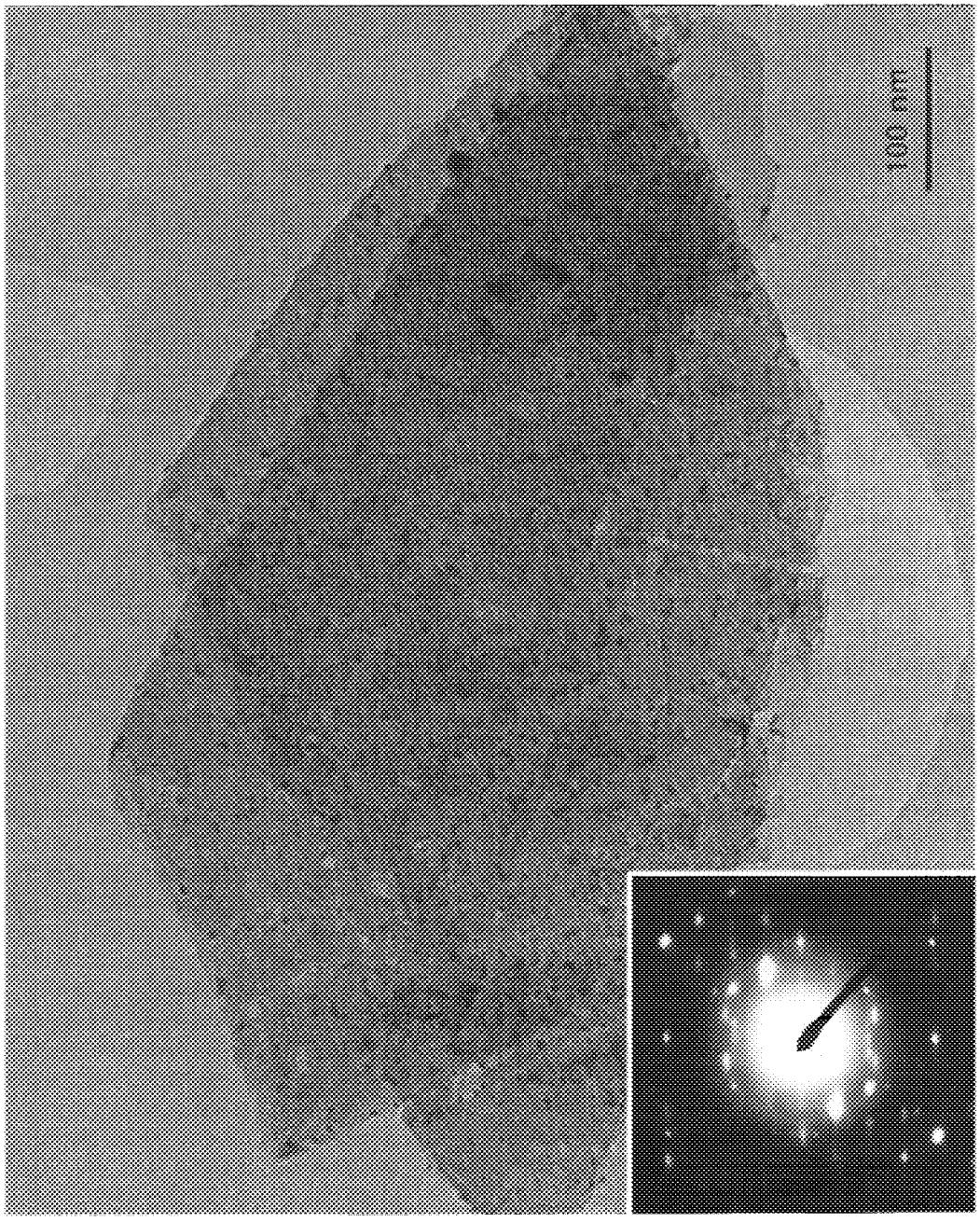
100 nm

factors. Interesting results were obtained by decreasing the diameter of the analyzed array. In the domains of small, isolated particles the promoter/platinum ratio was low as expected for submonolayer bismuth deposition. However, large fluctuations were measured in the agglomerates of 10–20 nm. Figure 6 represents an example on it. The average Bi/Pt atomic ratio of the catalyst was 0.06, but parts of the agglomerates contained almost pure bismuth. The agglomerates presumably contain small, originally isolated platinum particles covered by small amount of bismuth and bulk metallic bismuth "bridges" between them. There were no isolated bismuth particles on alumina.

We suggest that the formation of bulk bismuth crystallites between platinum particles is due to the presence of spilled-over hydrogen adatoms on the alumina support. The highest concentration of spilled-over hydrogen may be expected between the closely located platinum particles, in agreement with the picture obtained by electron microscopy.

Together with the investigations by means of HRTEM the analytical investigations lead to the conclusion that characteristically small amounts of bismuth are immobilized on platinum crystallites without forming a well defined alloy phase. Besides, there are clear indications that a fraction of bismuth promoter is deposited as bulk metal crystallites, closely connected with the Bi/Pt particles. The HRTEM-EDX analysis of lead-modified platinum on alumina catalysts lead to similar conclusions, though fluctuations in Pb/Pt ratio were observed in lower extent, which result is in a good agreement with that obtained for unsupported catalysts by cyclic voltammetry.

2. *Oxidation State of Promoters during Alcohol Oxidation*

It has been found earlier (*17*) that a dilute aqueous borax solution is the best solvent for the oxidation of 1-methoxy-2-propanol to methoxyacetone. However, even in this solution at 30°C the Pt on alumina catalyst quickly deactivates (Fig. 7). Bi, Pb, Sn, Au, and Ru promoters increase the conversion in this order. In general, an optimum in promoter/Pt_s ratio has been observed and the best results are plotted in Fig. 7. The initial rate of the oxidation reaction was found to be not significantly influenced by the catalyst composition (Fig. 8a). This behaviour is attributed to the oxygen transport being the rate-limiting step under these conditions. It has been proven earlier (*27–31*) that the rate of oxygen transport from the gas phase to the catalyst surface should be kept lower than that of the surface chemical reaction (alcohol oxidation) to avoid the over-oxidation of Pt^0 active sites. The promoters had only minor influence on the selectivity of the alcohol → ketone transformation, with the exception of Sn. Some examples are shown in Table 1. The characteristic side reaction occuring is the over-oxidation of the ketone product by C–C bond cleavage (*17*):

$$\begin{aligned} R\text{–}CH_2\text{–}CO\text{–}CH_3 + O_2 \rightarrow \\ R\text{–}COOH + R\text{–}CH_2COOH + \\ HCOOH + CH_3COOH + CO_2. \end{aligned} \quad (4)$$

Aldol dimerization and polymerization was found to be negligible in the absence of a strong base (NaOH) or carbon support.

The oxidation state of the promoters was followed by measuring the electrochemical potential of the catalyst during the oxidation of 1-methoxy-2-propanol (Fig. 8b). Before the oxidation reaction the catalysts were pre-reduced with hydrogen to obtain Pt^0 active sites. In the 0.1 *M* aqueous borax solution the potential of a platinum catalyst saturated with hydrogen is −0.75 V, referred to an $Ag/AgCl/KCl_{(sat)}$ electrode. The catalyst particles in the alkaline solution function as "short-circuited"

FIG. 4. High-resolution transmission electron micrograph of the 5 wt% platinum on alumina catalyst.


10 nm

cells, i.e., each platinum particle functions as an electrochemical cell, where both the anode and cathode half-reactions take place at the same rate and the same potential. After the addition of alcohol and introduction of air the catalyst potential quickly increases above 0 V. In the presence of alcohol the measured catalyst potential is a mixed potential determined by two or more electrode processes (*32, 33*). In the simplest case the two components are the alcohol oxidation reaction and the oxygen reduction reaction. Formally written:

$$\text{R–CH(OH)–R}'_{ad} + 2\text{OH}^- \rightarrow \text{R–CO–R}'_{ad} + 2\text{H}_2\text{O} + 2\text{e}^- \quad (5)$$

$$\tfrac{1}{2}\,\text{O}_2 + \text{H}_2\text{O} + 2\text{e}^- \rightarrow 2\,\text{OH}^-. \quad (6)$$

The redox potentials of various secondary alcohol → ketone reactions can be calculated from thermochemical data (*34*). The redox potential of the 1-methoxy-2-propanol → methoxyacetone transformation is −0.66 V vs the $Ag/AgCl/KCl_{(sat)}$ reference electrode. However, this value cannot be measured due to self-poisoning of the platinum (*35*). We tried to measure the rest potential of the Pt on alumina and the Bi-promoted Pt on alumina catalysts in the presence of a methoxy-propanol/methoxyacetone = 9 : 1 mixture. The catalysts were reduced with hydrogen, then the chemisorbed hydrogen was carefully oxidized and the alcohol/ketone mixture corresponding to 10% conversion and 100% selectivity was injected into the reactor, in a nitrogen atmosphere (Fig. 9). After a rapid potential drop the catalyst potential increased again and reached a broad maximum (~50 min), then slowly decreased. It has been found earlier (*36*) that the poison formation during methanol adsorption on polycrystalline platinum is a function of time as the adsorbates undergo transformations with time (*35*). The self-poisoning process depends on the catalyst material, which results in different electrochemical potentials of the promoted and unpromoted catalysts (Fig. 9). Similarly, a rest potential difference of 0.22 V was observed earlier during methanol adsorption on Pt and Pd (*37*).

If the platinum on alumina or any of the promoted catalysts were reduced with the 1-methoxy-2-propanol substrate itself in a nitrogen atmosphere, a rest potential of −0.3 V or less could not be reached. Performing this experiment with other secondary alcohols, such as diphenyl carbinol, 2-butanol, or 1-phenylethanol, the rest potentials were around −0.65 V. We suggest that the exceptionally strong self-poisoning with 1-methoxy-2-propanol is due to the strong influence of the electron-withdrawing α-methoxy group (*17*).

Comparing the curves of unpromoted platinum in Figs. 8b and 9, a potential difference of about 0.3–0.35 V can be calculated, which corresponds to the potential difference at 10% conversion measured in the absence and in the presence of air. In the case of the Bi-promoted catalyst this value is only 0.07–0.1 V. In the applied dilute aqueous borax solution hydrogen adsorbs on platinum in the region of −0.75/−0.30 V and OH adsorption becomes considerable above −0.15 V (Fig. 10, dashed line). The potential of the Pt on alumina catalyst between 3 and 17% conversion is (−0.02) − (+0.15 V) (Fig. 8b). Consequently, the catalyst is in an oxidized state during alcohol oxidation and its surface is partially covered by adsorbed OH. Promotion decreases the catalyst potential by up to 0.2 V, nevertheless, even in the best case the Bi–Pt bimetallic catalyst is partially oxidized after a few percent conversion. Note that there is practically no hydrogen on the surface of the cata-

FIG. 5. High-resolution transmission electron micrograph of a Bi–Pt/alumina catalyst; Bi/Pt_s = 0.20.

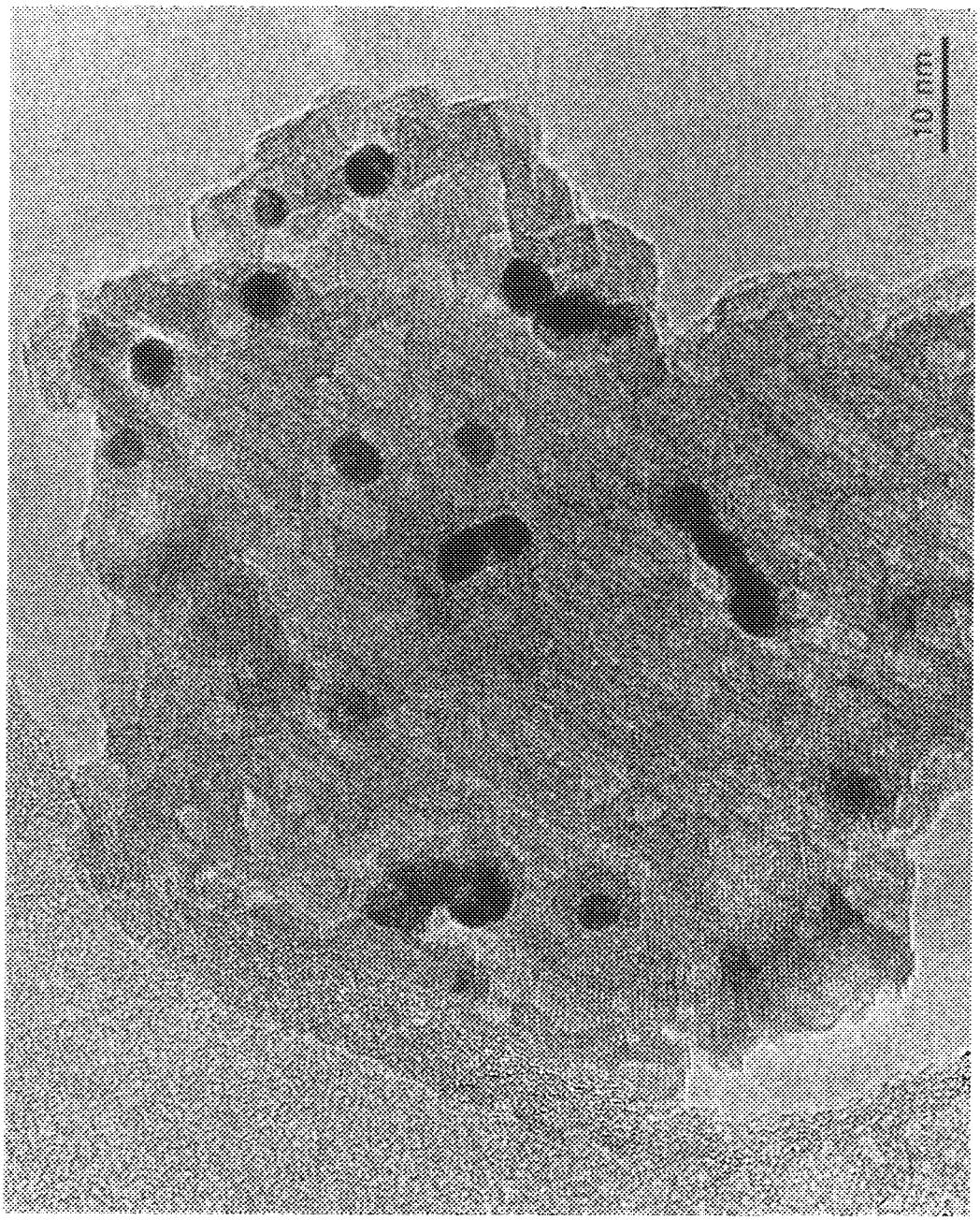
10 nm

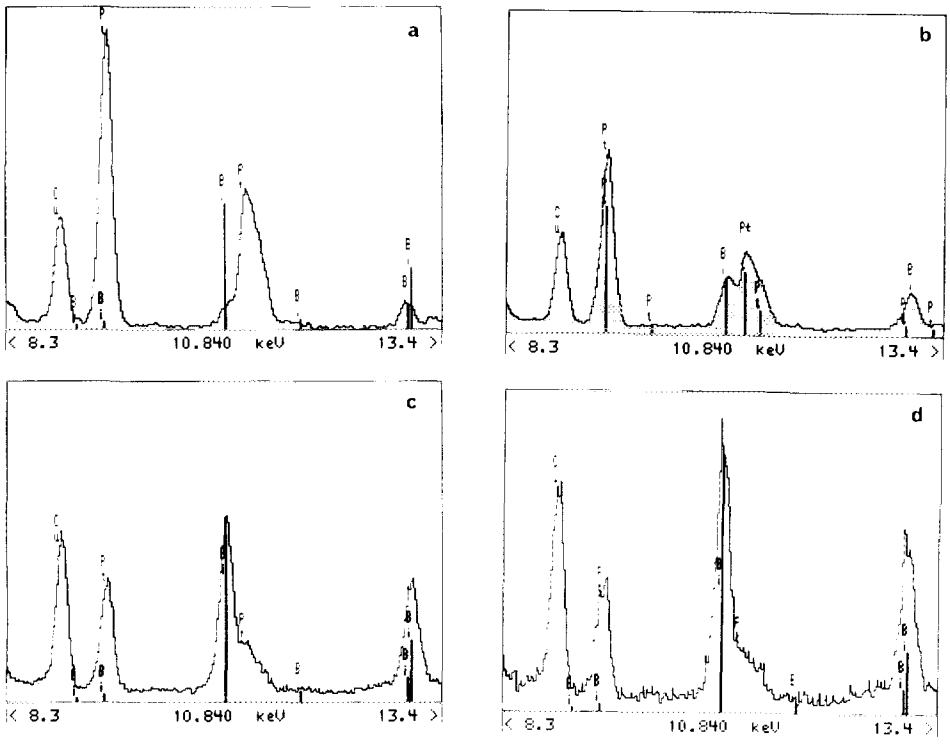

FIG. 6. Fluctuations in Bi/Pt ratio measured by STEM-EDX analysis of a Bi–Pt/alumina catalyst (Bi/Pt_s = 0.20); (a)–(d) increasing Bi/Pt ratio.

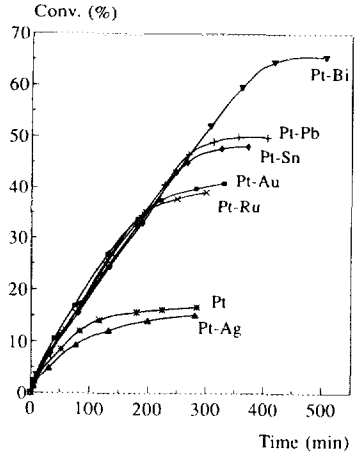

FIG. 7. Influence of promoters on the conversion of 1-methoxy-2-propanol; Bi/Pt_s = 0.20, Pb/Pt_s = 0.30, Sn/Pt_s = 0.13, Au/Pt_s = 0.26, Ru/Pt_s = 0.17, and Ag/Pt_s = 0.30.

lysts after the initial adsorption of methoxypropanol even in the absence of air, which is indicated by the potential above −0.3 V (Fig. 9).

We should note that in the literature (e.g., (*27*, *38*, *39*)) a relatively low catalyst potential has been observed in most cases. The generally accepted dehydrogenation mechanism is based on the presence of hydrogen on the catalyst surface during alcohol oxidation. The dehydrogenation of alcohol is supposed to be coupled with the oxidation of surface hydrogen with dioxygen either directly or by a local cell mechanism. We have also found that in the oxidation of many secondary alcohols like 2-propanol, 2-butanol, diphenyl carbinol, or 1-phenylethanol the catalyst potential is in the "hydrogen region" up to almost total conversion.

On the contrary, a partial oxygen coverage of the surface of a Pt on activated carbon

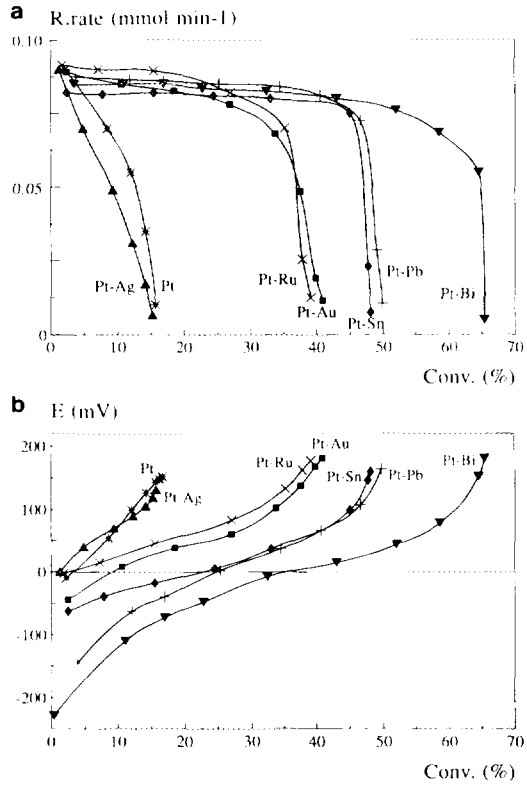

FIG. 8. The influence of promoters on the reaction rate (a) and on the electrochemical potential of the 5 wt% platinum on alumina catalyst (b) as a function of alcohol conversion; catalyst compositions are the same as those in Fig. 7.

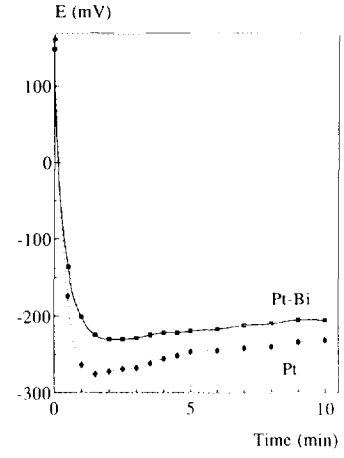

FIG. 9. Time dependence of the electrochemical potential of Pt on alumina and Bi-promoted Pt on alumina (Bi/Pt_s = 0.20) catalysts in a nitrogen atmosphere, in the presence of 1-methoxy-2-propanol/methoxyacetone = 9 : 1 molar mixture.

catalyst has been proven recently (*40–42*). A careful kinetic analysis of the selective oxidation of methyl α-D-glucoside to sodium 1-O-methyl α-D-glucuronate resulted in an oxygen coverage of Pt up to 0.8, depending on the reaction temperature and pH. The observed positive shift of the potential of the catalyst slurry within a few minutes after introduction of oxygen was explained by the oxygen chemisorption on platinum. A further increase of the catalyst potential during

TABLE 1

The Influence of Promotion on the Selectivity of Methoxy-propanol Oxidation

Promoter (M)	M/Pt_s (atom/atom)	Conversion (%)	Selectivity (%)
—	—	17	90
Pb	0.13	44	89
Pb	0.30	50	90
Bi	0.17	63	93
Bi	0.34	60	91
Sn	0.13	48	76
Sn	0.26	39	76

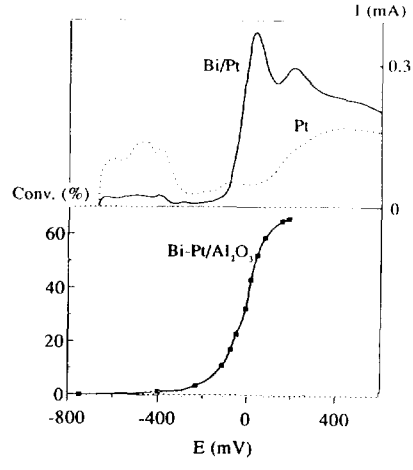

FIG. 10. Positive sweeps of the cyclic voltammograms of Pt (dashed) and Bi–Pt (continuous, θ_{Bi} = 0.85) powders and the potential of the Bi–Pt/alumina catalyst (Bi/Pt_s = 0.20) during the oxidation of 1-methoxy-2-propanol: scan rate: 1 m V · s^{-1}.

reaction was attributed to the almost complete coverage of platinum by oxygen, accompanied with its deactivation.

3. Role of Promoters

We suggest that the relative positive potential of the catalysts during reaction is due to the formation of strongly adsorbed by-products immediately after the addition of 1-methoxy-2-propanol. It means that the simplified picture of the mixed potential discussed above has to be completed with the side reaction(s). In situ spectroscopic measurements have shown that upon interaction of an alcohol with polycrystalline platinum a step-by-step dehydrogenation process occurs, resulting in the formation of strongly bound –CO, =CO and –CHO poisoning species (*35*, *43*). In situ electrochemically modulated IR spectroscopy (EMIRS) proved that the –CHO species are formed initially, and subsequently transform to linear and bridge bonded CO (*43*). Unfortunately, most of the literature data are concerned with the adsorption of small organic molecules, such as methanol, and there is a lack of information on the adsorption of higher alcohols.

It is supposed that the poison formation requires bigger active site ensembles than the alcohol oxidation reaction (*43*). An increase in the surface coverage of Pt by adatoms may suppress the formation of these by-products, resulting in an increase in the overall rate of alcohol oxidation. It is clear from Fig. 8 that this type of deactivation can be suppressed, but not eliminated, by promotion with heavy metals. Another frequently observed source of surface impurities is the aldol dimerization and polymerization of the product carbonyl compound catalyzed by strong bases and the basic functional groups of activated carbon, and a possible further oxidation of the dimer or polymer (*17*). This type of side reaction was found to be negligible in our case.

If the geometric blocking of active sites is the only source of promotion, then the deposition of promoter metals as isolated adatoms should have the highest influence on the catalytic performances (Fig. 1). The differences between the promoting effect of various heavy metals and also the negative influence of silver may be explained by the different surface geometry of the bimetallics. Silver adatoms may be located in big islands instead of scattered atoms and they cover only a fraction of surface active sites without influencing the size of active site ensembles. Unfortunately we could neither prove nor exclude this possibility. Investigations for elucidating this point are presently undertaken using scanning tunneling microscopy. *In situ* electrochemical scanning tunneling microscopic investigation on single crystal surfaces provided examples on both type of adatom deposition (*44*, *45*). Initial metal deposition may occur on surface dislocations, defects, and step edges, while preferential deposition in islands has also been observed.

The geometry of the active site ensembles is presumably influenced by the size of the adatoms and the number of active sites which they occupy. The latter values are 1 for Ag, 2 for Sn or Pb, and 3 for Bi (*46*). It is interesting that the higher is the site requirement of an adatom, the higher is its promoting effect. This positive correlation seems to be convincing, however, further experiments with several other type of adatoms would be necessary to confirm this hypothesis.

Another interpretation of the results is that Bi, Pb, Sn, Au, and Ru adatoms form new active centers, while Ag does not. Let us investigate the electrochemical potential of the promoted catalysts during alcohol oxidation in connection with the polarization curves of the corresponding (unsupported) bimetallic systems (Figs. 10–12). The interpretation of the positive sweeps of the cyclic voltammograms is similar to that of Pb-Pt curves shown in Fig. 2. Bismuth does not adsorb hydrogen and decrease the amount of hydrogen on platinum: the area under the polarization curve below -0.3 V is substantially smaller on the bimetallic catalyst (Fig.

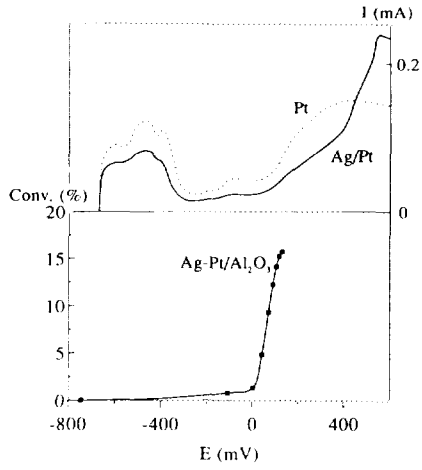

FIG. 11. Positive sweeps of the cyclic voltammograms of Pt (dashed) and Ag/Pt (continuous, θ_{Ag} = 0.40) powders and the potential of the Ag–Pt/alumina catalyst (Ag/Pt$_s$ = 0.30) during the oxidation of 1-methoxy-2-propanol; scan rate: 1 m V · s^{-1}.

10). The situation is the reverse in the "oxygen region": OH adsorption is considerably increased by the presence of promoter, due to its oxidation to $BiOH_{ad}$, than at higher potentials to BiO_{ad} and $Bi(OH)_{2,ad}$ (*47*). It is clear from the lower part of Fig. 10 that above 10% conversion of 1-methoxy-2-propanol the catalyst potential is just in the potential region where the promoter has the highest influence on the oxygen sorption characteristics of Pt. The lead- or tin-promoted platinum had similar hydrogen and oxygen sorption characteristics and their promotion influence was also similar but less efficient. On the contrary, silver adatoms decrease the OH adsorption on platinum in a broad potential range (Fig. 11), as the oxidation of silver adatoms occurs above 0.4 V.

We suggest that the promotion effect of bismuth, lead and tin adatoms is partially due to the formation of new active centers, which adsorb OH better than platinum:

$$Pt\text{–}M_{ad} + OH^- \rightarrow Pt\text{–}M_{ad}\text{–}OH + e^-. \quad (7)$$

The alcohol substrate can adsorb on Pt^0 sites (and on alumina). A formal reaction mechanism may be suggested according to which the adsorbed OH radicals react with an (unknown) alcohol adsorption intermediate. The reaction rate may formally be written as

$$r = f \cdot \theta_{org} \cdot \theta_{OH}. \quad (8)$$

A maximum in reaction rate has been observed at medium coverage of Pt by Bi, Pb, Sn, Au, and Ru adatoms, expectedly. There are several examples in the literature on this type of rate equation for alcohol oxidation derived from kinetic analysis of the reaction. Examples are the catalytic oxidation of D-gluconate or methyl α-D-glucoside on Pt/C (*29, 42*), the electrocatalytic oxidation of methanol (*48*), ethylene-glycol (*25*) or 1,2-propanediol (*49*) on polycrystalline Pt modified with Ru, Bi, Pb, Cd, Cu, or Tl adatoms. The role of gold seems to be ambiguous. OH adsorption on Au adatoms and bifunctional catalysis was suggested earlier (*50*), but we found that Au adatoms on unsupported platinum slightly decrease the oxygen sorption in the potential region of 1-methoxy-2-propanol oxidation, in accordance with the latest data (*51*).

The promotion with ruthenium resulted in the smallest increase in conversion (Fig. 7), though the OH sorption is considerably higher on ruthenium-promoted platinum than on platinum in a broad potential range (Fig. 12). The substantial difference between ruthenium and bismuth, lead, tin, or gold adatoms is that only ruthenium adsorbs hydrogen. The decrease of hydrogen sorption on platinum may be important in the by-product formation during alcohol adsorption. The involvement of adsorbed hydrogen in the poison formation reaction is one of the current conceptions for the explanation of the role of adatoms in the electrooxidation of small organic molecules (*35*).

Summarizing the results we may conclude that the bimetallic catalysts are in an oxidized state during the partial oxidation of 1-methoxy-2-propanol. The positive shift in the electrochemical potential of the catalyst

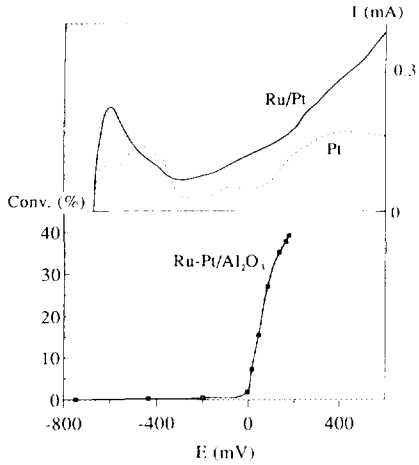

FIG. 12. Positive sweeps of the cyclic voltammograms of Pt (dashed) and Ru/Pt (continuous) powders and the potential of the Ru/Pt/alumina catalyst (Ru/Pt_s = 0.17) during the oxidation of 1-methoxy-2-propanol; scan rate: 1 m V · s^{-1}.

slurry observed after introduction of the substrate and air into the reactor is explained by an irreversible adsorption of the alcohol substrate and a partial oxygen (OH) coverage of the bimetallics. A further, moderate increase of the catalyst potential close to the end of the reaction is due to the complete coverage of the catalyst with oxygen, accompanied with its deactivation. We suggest that the best promoters, Bi and Pb, act in two ways. They suppress the irreversible adsorption of alcohol (self-poisoning) on Pt and form new active centers, which adsorb OH better than Pt in the potential range where the oxidation reaction occurs.

ACKNOWLEDGMENTS

Financial support of this work by Sandoz AG, Switzerland is gratefully acknowledged. Thanks are also due to Engelhard, Netherlands for supplying the platinum on alumina catalyst.

REFERENCES

1. Fiege, H., and Wedemeyer, K., *Angew. Chem.* **93,** 812 (1981).
2. Smits, P. C. C., Kuster, B. F. M., van der Wiele, K., and van der Baan, H. S., *Carbohydr. Res.* **153,** 227 (1986).
3. Smits, P. C. C., Kuster, B. F. M., van der Wiele, K., and van der Baan, H. S., *Appl. Catal.* **33,** 83 (1987).
4. Despevroux, B. M., Deller, K., and Peldszus, E., *in* "New Developments in Selective Oxidation" (G. Centi and F. Trifiro, Eds.), Studies in Surface Science and Catalysis, Vol. 55, p. 159. Elsevier, Amsterdam, 1990.
5. Hronec, M., Cvengrosova, Z., Tuleja, J., and Ilavsky, J., *in* "New Developments in Selective Oxidation" (G. Centi and F. Trifiro, Eds.), Studies in Surface Science and Catalysis, Vol. 55, p. 169. Elsevier, Amsterdam, 1990.
6. Hendriks, H. E. J., Kuster, B. F. M., and Marin, G. B., *Carbohydr. Res.* **204,** 121 (1990).
7. Li, Z. M., and Zhang, M. Z., *J. Catal. (China)* **11,** 106 (1990), from *Plat. Met. Rev.* **34,** 230 (1990).
8. van Bekkum, H., *in* "Carbohydrates as Organic Raw Materials" (F. W. Lichtenthaler, Ed.), p. 289. VCH, Weinheim, 1990.
9. Muroi, T., *Chem. Catal. News (Engelhard)*, March (1991).
10. Mallat, T., and Baiker, A., *Appl. Catal. A: Gen.* **79,** 41 (1991).
11. Mallat, T., Baiker, A., and Patscheider, J., *Appl. Catal. A: Gen.* **79,** 59 (1991).
12. Mallat, T., Allmendinger, T., and Baiker, A., *Appl. Surf. Sci.* **52,** 189 (1991).
13. Tsujino, T., Ohigashi, S., Kawashiro, K., and Hayashi, H., *J. Mol. Catal.* **71,** 23 (1992).
14. Vinke, P., de Wit, D., de Goede, A. T. J. W., and van Bekkum, H., *in* "New Developments in Selective Oxidation by Heterogeneous Catalysis" (P. Ruiz and B. Delmon, Eds.), Studies in Surface Science and Catalysis, Vol. 72, p. 1. Elsevier, Amsterdam, 1992.
15. Sokolskii, D. V., "Hydrogenation in Solutions." Izd. Nauka Kaz. SSR, Alma Ata (1979). [in Russian]
16. Woods, R., *in* "Electroanalytical Chemistry" (A. J. Bard, Ed.), Vol. 9, p. 1. Dekker, New York, 1976.
17. Mallat, T., Baiker, A., and Botz, L., *Appl. Catal. A.: Gen.* **86,** 147 (1992).
18. Mallat, T., and Petro, J., *React. Kinet. Catal. Lett.* **11,** 307 (1979).
19. Baria, D. N., and Hulburt, H. M., *J. Electrochem. Soc.* **120,** 1333 (1973).
20. van der Plas, J. F., Barendrecht, E., and Zeilmaker, H., *Electrochim. Acta* **25,** 1471 (1980).
21. Kolb, D. M., *Adv. Electrochem. Electrochem. Eng.* **11,** 125 (1978).
22. Szabo, S., *Int. Rev. Phys. Chem.* **10,** 207 (1991).
23. Muhler, M., Paal, Z., and Schlögl, R., *Appl. Surf. Sci.* **47,** 281 (1991).
24. Angerstein-Kozlowska, H., Conway, B. E., Barnett, B., and Mozota, J., *J. Electroanal. Chem.* **100,** 417 (1979).
25. Kadirgan, F., Beden, B., and Lamy, C., *Electroanal. Chem.* **143,** 135 (1983).

26. Amadelli, R., Molla, J. A., and Yeager, E., *J. Electroanal. Chem.* **126,** 265 (1981).
27. Dirkx, J. M. H., and van der Baan, H. S., *J. Catal.* **67,** 1 (1981).
28. Dirkx, J. M. H., and van der Baan, H. S., *J. Catal.* **67,** 14 (1981).
29. Dijkgraaf, P. J. M., Rijk, M. J. M., Meuldijk, J., and van der Wiele, K., *J. Catal.* **112,** 329 (1988).
30. Dijkgraaf, P. J. M., Duisters, H. A. M., Kuster, B. F. M., and van der Wiele, K., *J. Catal.* **112,** 337 (1988).
31. Vinke, P., van der Poel, W., and van Bekkum, H., *in* "Heterogeneous Catalysis and Fine Chemicals II" (M. Guisnet *et al.*, Eds.), Studies in Surface Science and Catalysis, Vol. 57, p. 385. Elsevier, Amsterdam, 1991.
32. Wagner, C., and Traud, W., *Z. Electrochem.* **44,** 391 (1938).
33. Koryta, J., and Dvorak, J., "Principles of Electrochemistry," Wiley, Chichester, 1987.
34. Perry, R. H., Green, D. W., and Maloney, J. O., "Perry's Chemical Engineers' Handbook," McGraw-Hill, New York, 1984.
35. Parsons, R., and VanderNoot, T., *J. Electroanal. Chem.* **257,** 9 (1988).
36. Hughes, V. B., and Miles, R., *J. Electroanal. Chem.* **145,** 87 (1983).
37. Van Dam, H. E., Wisse, L. J., and van Bekkum, H., *J. Catal.* **61,** 187 (1990).
38. Nicoletti, J. M., and Whitesides, G. M., *J. Phys. Chem.* **93,** 759 (1989).
39. DiCosimo, R., and Whitesides, G. M., *J. Phys. Chem.* **93,** 768 (1989).
40. Schuurman, Y., Kuster, B. F. M., van der Wiele, K., and Marin, G. B., *in* "New Developments in Selective Oxidation by Heterogeneous Catalysis" (P. Ruiz and B. Delmon, Eds.), Studies in Surface Science and Catalysis, Vol. 72, p. 43. Elsevier, Amsterdam, 1992.
41. Schuurman, Y., Kuster, B. F. M., van der Wiele, K., and Marin, G. B., *Appl. Catal. A: Gen.* **89,** 31 (1992).
42. Schuurman, Y., Kuster, B. F. M., van der Wiele, K., and Marin, G. B., *Appl. Catal. A: Gen.* **89,** 47 (1992).
43. Christensen, P. A., and Hamnett, A., *in* "Chemical Kinetics" (R. G. Compton and A. Hamnett, Eds.), Vol. 29, p. 28. Elsevier, Amsterdam, 1989.
44. Cataldi, T. R. I., Blackham, I. G., Briggs, G. A. D., Pethica, J. B., and Hill, H. A. O., *J. Electroanal. Chem.* **290,** 1 (1990).
45. Nichols, R. J., Kolb, D. M., and Behm, R. J., *J. Electroanal. Chem.* **313,** 109 (1991).
46. Furuya, N., and Motoo, S., *J. Electroanal. Chem.* **98,** 189 (1979).
47. Clavilier, J., Feliu, J. M., and Aldaz, A., *J. Electroanal. Chem.* **243,** 419 (1988).
48. Watanabe, M., and Motoo, S., *J. Electroanal. Chem.* **60,** 267 (1975).
49. Ocon, P. Beden, B., and Lamy, C., *Electrochim. Acta* **32,** 1095 (1987).
50. Watanabe, M., and Motoo, S., *J. Electroanal. Chem.* **60,** 259 (1975).
51. Bakos, I., and Szabo, S., *J. Electroanal. Chem.* **344,** 303 (1993).